

Biosolids-based catalyst for oxidative desulphurization of drop-in fuels derived from waste fats

*Original*

Biosolids-based catalyst for oxidative desulphurization of drop-in fuels derived from waste fats / Bartoli, M., Zhu, C., Asomaning, J., Chae, M., Bressler, D.C.. - In: FUEL. - ISSN 0016-2361. - ELETTRONICO. - 324A:(2022), p. 124546. [10.1016/j.fuel.2022.124546]

*Availability:*

This version is available at: 11583/2965073 since: 2022-05-30T13:25:53Z

*Publisher:*

Elsevier Ltd

*Published*

DOI:10.1016/j.fuel.2022.124546

*Terms of use:*

This article is made available under terms and conditions as specified in the corresponding bibliographic description in the repository

*Publisher copyright*

(Article begins on next page)



## Full Length Article

# Biosolids-based catalyst for oxidative desulphurization of drop-in fuels derived from waste fats

Mattia Bartoli, Chengyong Zhu, Justice Asomaning, Michael Chae, David C. Bressler\*

Department of Agricultural, Food and Nutritional Science, University of Alberta, 410 Ag/For Building, Edmonton, AB T6G 2P5, Canada



## ARTICLE INFO

## Keywords:

Catalytic desulphurization  
Drop-in fuel  
Biosolids  
Pyrolysis

## ABSTRACT

In this work, the catalytic performance of a biosolids-based catalyst was tested in the oxidative desulphurization process of a model fuel solution containing benzothiophene ([S] of 500 ppm), as well as sulphur-rich products from a two-step thermal conversion process of brown grease to renewable hydrocarbons using biosolids as a water replacement during the hydrolysis step. The catalytic results of the biosolids-based material were compared with a classical Fenton-like reagent and a non-catalytic system. Biosolids-based catalyst outperformed the other systems at low temperature with a full desulphurization of benzothiophene solution achieved at 60 °C after 3 h and a good recyclability after four catalytic runs at 80 °C for 3 h. The desulphurization was less effective for hydrolysed fatty acids and crude pyrolysis oil derived from the conversion of brown grease to renewable hydrocarbons, which was due to the composition of the sulphur containing compounds, but still reached  $87.7 \pm 3.0\%$  and  $74.7 \pm 9.5\%$ , respectively.

## 1. Introduction

The overall demand of water for human activities and the amount of wastewater produced are continuously increasing worldwide year by year [1]. Wastewater management has become one of the major priorities for every urban conglomerate, involving several biological and chemical treatments [2] to facilitate reuse in civilian and industrial applications. Wastewater treatments lead to the formation of a semisolid residue called sewage sludge [3] that can be used only after several additional treatments. According to the USEPA's definition [4], biosolids are the final residue from properly treated sewage sludge. Biosolids are composed mostly of water (90–95 wt%), with a small percentage of solids (up to 5 wt%) [5]. The organic fraction represents the 40–60 wt% of the solid residue and it is composed of sugars (up to 20 wt%), lipids (10–15 wt%), proteinaceous derivatives (30–60 wt%) [6] and small organic molecules such as polyphenols and pharmaceutical residues [7,8]. The inorganic fraction contains sand and heavy metals (*i.e.* Fe, Cr, Mo, Zn, Al, Cu, Sn, Ag, Ti and traces of others [9,10]).

The global annual biosolids production is estimated at around the 3 trillion tonnes [11] and despite their applications in agriculture [12] and landscaping [13], 30–40 wt% of total biosolids is currently disposed of through artificial lagoons [14]. To avoid the use of such high environmental impact disposal routes, biosolids have been used as feedstocks

for several conversions processes, both biological [15] and thermochemical [16,17]. Recently, biosolids were incorporated as a water replacement into a two-step thermal conversion process capable of generating renewable hydrocarbons from wasted fats and oils [18]. This conversion route allows to remove oxygenated compounds formed from the cracking of glycerol contained into waster fatty.

As reported by Omidghane et al. [18], fuel produced from a two-step lipid pyrolysis process incorporating biosolids contained sulphur at levels higher than allowable for their direct use in common engines. This was attributed to the presence of sulpholipids, proteinaceous residues, and organic sulphur contained in biosolids. As shown by Bartoli et al. [19], a non-catalytic integrated approach could be used to decrease sulphur levels of this fuel stream derived from brown grease and biosolids to  $15 \pm 4$  ppm. However, this non-catalytic approach required several steps due to the composition of the sulphur compounds present in the mixture treated. In order to meet the sulphur limits for transportation fuels [20], several authors have proposed a general catalytic oxidative procedure that could be used to convert any organic sulphur species into hydrosoluble sulfone species, which could then be extracted in polar solvents [21]. Catalytic oxidative desulphurization can be performed using several transition metal-based catalysts (*i.e.* Co [22], W [23], Mn [24], Fe [25] or polyoxometalates [26]), molecular oxygen [27,28] or peroxides as oxidizing agents [29–31], and different solvents

\* Corresponding author.

E-mail address: [david.bressler@ualberta.ca](mailto:david.bressler@ualberta.ca) (D.C. Bressler).

<https://doi.org/10.1016/j.fuel.2022.124546>

Received 22 February 2022; Received in revised form 4 May 2022; Accepted 6 May 2022

Available online 13 May 2022

0016-2361/© 2022 The Authors. Published by Elsevier Ltd. This is an open access article under the CC BY-NC-ND license (<http://creativecommons.org/licenses/by-nc-nd/4.0/>).

[32–34]. Among all available catalysts, iron-based catalysts are very attractive because of their low cost and the possibility to perform a Fenton or a Fenton-like reaction [35], enhancing the oxidative power of  $\text{H}_2\text{O}_2$  [36].

Biosolids can contain a high concentration of iron species caused by the addition of iron salts as coagulants during the treatment of sewage sludge [37]. As observed by Xia et al. [38], a thermal hydrolytic treatment induced a rapid sedimentation of biosolids with the formation of a metals-rich material. The solid residue recovered from hydrolysed biosolids has been shown to be an active catalyst for several applications [39,40].

In this study, the solid residue remaining after thermal hydrolysis of biosolids was used as catalyst for oxidative desulphurization procedures. The activity of this catalyst was compared with a classical Fenton-like catalyst ( $\text{FeCl}_3$ ) and with a non-catalytic system for the desulphurization of a model fuel solution containing benzothiophene using  $\text{H}_2\text{O}_2$ . The catalytic performance of the metals-rich residue recovered after the hydrolysis of biosolids were also investigated using the lipid phase recovered after hydrolysis of brown grease using biosolids as a water replacement, as well as crude pyrolysis oil obtained using this lipid phase as feedstock for pyrolysis.

## 2. Materials and methods

### 2.1. Materials

1 kg of biosolids (supplied by a Wastewater treatment facility in Edmonton, Canada.) were used to hydrolyze 1 kg of brown grease using a pressurized 5.5 L reactor (Model 4580, Parr Instrument Company, Moline, IL, USA) at 280 °C for 60 min according to the procedure reported by Xia et al. [38]. The solid residue formed during the hydrolysis was collected and dried to a constant weight in an oven at 105 °C and then manually ground using a mortar and pestle. Crude pyrolysis oil was produced using a 1 L batch mechanical stir reactor (Parr Instrument Co., Moline IL) at 410 °C for 1 h using a procedure previously reported by Asomaning et al. [41].

A model fuel solution containing 500 ppm of sulphur was prepared dissolving 370 mg of benzothiophene in 250 mL of heptane. Pentane (HPLC grade, >99.9%), heptane (HPLC grade, >99.9%) and methyl nonadecanoate (used as internal standard for gas chromatography of the liquid products) were purchased from Sigma-Aldrich (St. Louis, MO, USA). Diazomethane for derivatization of fatty acids was prepared using a Diazald kit (Sigma-Aldrich, St. Louis, MO, USA) according to the procedures supplied by the manufacturer. Diazald (N-Methyl-N-nitroso-p-toluenesulfonamide) used for the preparation of diazomethane was purchased from TLC PharmaChem Inc (Concord, ON, Canada).  $\text{H}_2\text{O}_2$  (30%), benzothiophene,  $\text{FeCl}_3 \cdot (\text{H}_2\text{O})_6$ , and acetic acid (98%) were purchased from Sigma-Aldrich (St. Louis, MO, USA). Gases (Air,  $\text{N}_2$ ,  $\text{H}_2$ , He) were purchased from Praxair (Praxair Inc., Edmonton, AB).

### 2.2. Methods

#### 2.2.1. Catalytic oxidative desulphurization procedures

2 mL of sulphur containing model fuel was prepared by Model fuel (500 ppm of sulphur concentration), 2 g of hydrolysed fatty acids or 2 mL of crude pyrolysis oil were put in a plastic tube with  $\text{H}_2\text{O}_2$  ( $\text{H}_2\text{O}_2/\text{sulphur} = 10/1$  mol), 3.7 mL of  $\text{H}_2\text{O}$ , 0.3 mL and acetic acid (98%) and  $\text{FeCl}_3(\text{H}_2\text{O})_6$  ( $\text{Fe}/\text{sulphur} = 0.05$  mol/mol) and then sealed. The same procedure was employed using the solid recovered after hydrolysis of biosolids ( $\text{Fe}/\text{sulphur} = 0.05$  mol/mol) or without any catalyst addition. Solutions were stirred and heated at different temperatures (50 °C, 60 °C, 70 °C, 80 °C) for different times (15 min, 30 min, 60 min, 120 min, 180 min) in an oil bath. Afterwards, the solutions were allowed to cool to room temperature in air and 5 mL of water were added. The upper organic phases were recovered and analyzed. The biosolids-based catalyst was recovered after catalysis through centrifugation ( $7155 \times g$

for 10 min), dried overnight at 105 °C and then analyzed. Each test was replicated three times.

#### 2.2.2. Samples analysis

Before and after any oxidative catalytic desulphurization treatments, the hydrolysed fatty acids mixture and crude pyrolysis oil were analyzed through gas chromatography to determine their compositions. In each case, 100 mg of each sample were diluted in 0.5 mL of pentane, with the addition of 25 mg of methyl decanoate as the internal standard. After this, 100  $\mu\text{L}$  of the solution were diluted with 0.5 mL of diazomethane solution in order to produce fatty acids methyl esters. The final solutions were analyzed using a gas chromatograph (6890 N, Agilent Technologies, Fort Worth, TX) equipped with an autosampler (Agilent 7683 series; Agilent Technologies, Fort Worth, TX), an FID and mass spectrometer (Agilent 5975B inert XL EI/CI MSD; Agilent Technologies, Fort Worth, TX). Analysis were carried out via injection of 1  $\mu\text{L}$  of the samples onto a DB-5 column (100 m  $\times$  250  $\mu\text{m}$   $\times$  0.25  $\mu\text{m}$ ; Agilent Technologies, Fort Worth, TX) according to a procedure previously described [18].

1 mL of model fuel solution containing benzothiophene in heptane that was recovered after each catalytic test was also analyzed through addition of 5 mg of methyl nonadecanoate as the internal standard and using the same chromatographic procedure described above. The concentration of benzothiophene after catalysis was evaluated using a five-point calibration curve ( $m = 1.029 \pm 0.006$ ,  $R^2 = 0.999$ ) obtained using methyl nonadecanoate as the internal standard. It is worth noting that oxidized species as well as other sulphur containing compounds were not observed when the oxidized model fuel was analyzed on GC. As such, the conversion of benzothiophene was equated to desulphurization.

Sulphur concentrations in the hydrolysed fatty acids and crude pyrolysis oil prior to and after the catalytic desulphurization process were evaluated through ICP-OES, which was performed by the Natural Resources Analytical Laboratory (Department of Chemistry, University of Alberta) using a ThermoCAP6000 series inductively coupled plasma-optical emission spectrometer (Fisher Thermoscientific, Cambridge, United Kingdom) according to a procedure previously described [19].

The composition of the inorganic residues within the solid material recovered after hydrolysis of biosolids at 280 for 1 h was evaluated after incineration of 5 g of the sample at 450 °C for 6 h using a 48,000 Furnace (Barnstead Thermolyne, Dubuque, Iowa, USA) according to methodology reported by Benitez et al. [42]. FT-IR ATR analyses were carried out at the Nanofabrication and characterization facility, University of Alberta, using a Nicolet Is-50 (Thermoscientific, Madison, WI, USA) in the range of 4000–600  $\text{cm}^{-1}$  with a band of resolution of 2  $\text{cm}^{-1}$ .

#### 2.2.3. Statistical analysis

ANOVA tests with a significance level of 0.05 ( $p < 0.05$ ) were performed using Excel™ software (Microsoft Corp.) and the “Data analysis” plug-in.

## 3. Results

### 3.1. Preliminary considerations about the solid recovered after hydrolysis of biosolids at 280 °C for 1 h

Selective metals recovery from biosolids is a challenging process because of the extremely high water content and the organic materials (*i.e.* phenols, sugars, proteinaceous materials) remaining after sewage sludge treatments. Hydrolysis at high temperature (280 °C) for 1 h has proven to be a very efficient way to induce a very rapid sedimentation of biosolids [38], promoting the accumulation of metals in the solid residue as shown in Table 1. The solid residue recovered after the hydrolysis of biosolids contained high amount of iron ( $26.5 \pm 1.3$  mg/g) and aluminum ( $26.85 \pm 1.34$  mg/g), but zinc ( $1.06 \pm 0.05$  mg/g) and titanium ( $3.21 \pm 0.16$  mg/g) were also detected in appreciable concentrations.

**Table 1**

Main metals detected in the solid recovered after hydrolysis of biosolids (a) before catalysis and b) after the third desulphurization cycle of a benzothiophene solution at 80 °C for 3 h. The standard deviations of triplicate experiments are reported.

	Concentration [mg/g]									
	Cr	Fe	Mn	Sn	Al	Cu	Zn	Pb	Ti	Si <sup>a</sup>
As reported by Bartoli et al. [39]	0.39 ± 0.02	26.5 ± 1.33	0.58 ± 0.03	0.37 ± 0.02	26.9 ± 1.34	0.71 ± 0.04	1.06 ± 0.05	0.10 ± 0.01	3.21 ± 0.16	112 ± 14
After 3 catalytic runs	0.40 ± 0.02	28.7 ± 1.69	0.36 ± 0.02	0.39 ± 0.02	25.2 ± 1.60	0.22 ± 0.01	0.72 ± 0.04	0.16 ± 0.01	0.13 ± 0.01	137 ± 13

a) Calculated by difference on inorganic fraction of biosolid based catalyst.

The metals detected were dispersed into a complex matrix composed of both organic and inorganic components. The inorganic fraction represented  $30.3 \pm 0.6$  wt% and, according to the XRPD analysis reported in Fig. 1, silica (sodalite  $\text{Si}_{12}\text{O}_{24}$ ) is the most abundant species, though several other metal species were detected:  $\text{Fe}_3\text{O}_4$ ,  $\text{FeOOH}$ ,  $\text{Fe}_2(\text{SO}_4)_3$ ,  $\text{FePO}_4$ ,  $\text{Al}_2\text{O}_3$ ,  $\text{TiO}_2$ , and  $\text{CuS}$ .

The metals reported in Table 1 are able to promote the activation of  $\text{H}_2\text{O}_2$  under several conditions as soluble species or supported materials [43]. Heterogeneous catalysts based on iron [44] and aluminium [45] have been largely studied and a clear relationship between acid sites on the support surface and the enhancement of catalytic exploits has emerged. The large amount of silica-like materials likely result from the accumulation of sandstone residues during the sedimentation of biosolids.

Despite this, the organic matter (around the 70 wt%) displayed limited acidic functionalities as evident from the low intensity bands of carboxylic functionalities ( $\nu_{\text{O-H}}$   $3380\text{ cm}^{-1}$ ,  $\nu_{\text{C=O}}$   $1780\text{--}1680\text{ cm}^{-1}$ ) shown in the FT-IR analysis (Fig. 2). The main bands detected were  $\nu_{\text{O-H}}$  ( $3380\text{ cm}^{-1}$ ),  $\nu_{\text{C-H}}$  ( $3237, 2923\text{--}2825\text{ cm}^{-1}$ ) of unsaturated and saturated hydrocarbons,  $\nu_{\text{C=C}}$  ( $1640\text{ cm}^{-1}$ ),  $\delta_{\text{C-H in plane}}$  ( $1420\text{ cm}^{-1}$ ) of unsaturated hydrocarbons,  $\delta_{\text{C-O}}$  ( $1051\text{--}995\text{ cm}^{-1}$ ),  $\delta_{\text{C-H out of plane}}$  ( $797\text{--}696\text{ cm}^{-1}$ ) of unsaturated hydrocarbons. It is possible to argue a considerable presence of aromatic compounds from their characteristic bands (i.e.  $\nu_{\text{C=C}}$ ,  $\delta_{\text{C-H in plane}}$ ). Also, the strong signals of  $\delta_{\text{C-H out of plane}}$  suggest that the aromatics are variously substituted. From these data, it is reasonable to suppose that the organic matrix of the solid recovered after the hydrolysis of biosolids is composed for the most by polycyclic aromatic compounds. Those compounds could be formed through radical rearrangement during hydrolytic treatment of biosolids from the polycyclic aromatics detected by several authors [46,47]. Hydrosoluble species (hydrolysed proteinaceous materials, sugars, and small fatty

acids) were reasonably retained in the aqueous phase. Thus, the lack of acidic sites could be balanced by the presence of extended aromatic systems that could promote radical stabilization as in the case of carbon nanotube-based catalysts [48].

### 3.2. Comparative catalytic studies using a model fuel solution of benzothiophene in heptane

After the treatment of biosolids (i.e. addition of Fe(III) as flocculating agents, aerobic digestion, thermal hydrolysis), iron species are present in the solid residue mostly as high oxidation state Fe(III), based on the species detected using XRPD technique (see Fig. 1). Thus, the solid recovered after hydrolysis of biosolids was tested as catalyst for oxidative desulfurization and compared with  $\text{FeCl}_3$ , a classical Fenton-like reagent in a biphasic system with desulphurization routes as those shown in Fig. 3.

Fenton and Fenton-type reactions are based on the simultaneous use of iron salts and  $\text{H}_2\text{O}_2$  to produce highly reactive oxygen radical species according to Pignatello et al. [49]. The catalysts for Fenton reactions are Fe(II) species but the mechanism reported by Barb et al. [50] involves the production of Fe(III) and several equilibria between Fe(II)/Fe(III). Fenton-type reactions are similar but instead of Fe(II) the starting iron specie is Fe(III) [51] and the initial step of activation of water involves the formation of a different intermediate ( $[\text{Fe}^{\text{III}}\text{OOH}]^{2+}$ ) [52]. As reported by Ruipérez et al. [53], the presence of aluminum species could enhance the activity of iron species through the mechanism reported in Fig. 4. Furthermore, the presence of other metals such as copper and titanium together with abundant silica could further boost the catalytic activity of iron centers [54].

Among all Fe(III) salts,  $\text{FeCl}_3$  was chosen because Fe(III) halides are less reactive than others species and do not degrade the aromatic moieties [55], preventing the loss of aromatics during the treatment of fuels. Despite this, iron halides require an acidic environment to prevent the formation of insoluble species during the process [49,56]. Acetic acid was added to set the pH of the aqueous phase below 4, ensuring the solubility of iron species and enhancing the oxidative power of the system with the in-situ formation of peracetic acid [57].

Comparisons between the biosolid-based catalyst and  $\text{FeCl}_3$  was not a simple task because of the presence of other metals in the solid recovered after the hydrolysis of biosolid that can also promote the activation of  $\text{H}_2\text{O}_2$ . Thus, the total amount of iron in the biosolid-based catalyst was chosen as the referenced parameter, using a Fe/sulphur ratio of 0.05 mol/mol in each catalytic run as reported in Table 2.

According to two-way Anova tests, both temperature and time affected the conversion of all systems ( $p < 0.05$ ). Considering the non-catalytic system, temperature played the most relevant role ( $F = 3543.8$ ,  $F_{\text{crit}} = 2.8$ ) compared with time ( $F = 1680.1$ ,  $F_{\text{crit}} = 2.6$ ); a similar trend was observed using the solid recovered after hydrolysis of biosolids as catalyst (time outputs:  $F = 1991.7$ ,  $F_{\text{crit}} = 2.8$ ; temperature outputs:  $F = 1640.1$ ,  $F_{\text{crit}} = 2.6$ ). In contrast,  $\text{FeCl}_3$  activity was affected more by the temperature increments ( $F = 5765.2$ ,  $F_{\text{crit}} = 2.8$ ) than from increasing time ( $F = 532.4$ ,  $F_{\text{crit}} = 2.6$ ).

Using the solid recovered after hydrolysis of biosolids, a nearly complete conversion was observed after 3 h at 60 °C; under the same

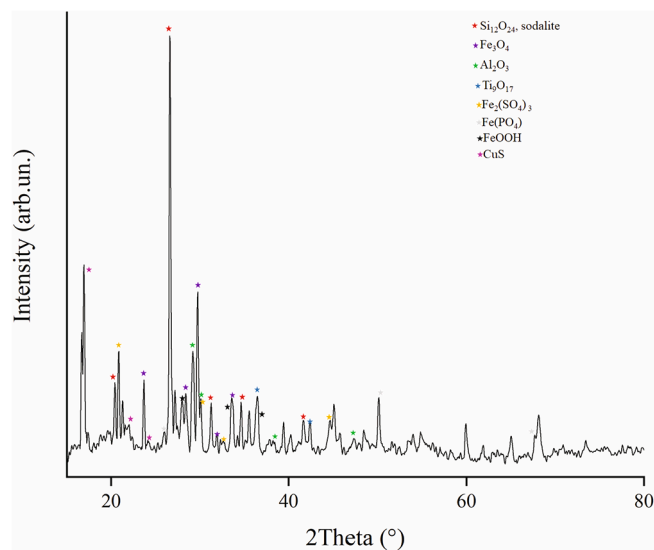


Fig. 1. XRPD analysis of the solids recovered after hydrolysis of biosolids at 280 °C (before catalysis) in the range of 15–80 2 $\theta$ .



**Table 2**

Comparison of the performance of solid recovered after the hydrolysis of biosolids at 280 °C for 1 h, FeCl<sub>3</sub> and H<sub>2</sub>O<sub>2</sub> without any addition of catalyst in the desulphurization of a benzothiophene solution in heptane. The data represent mean ± standard deviation with n = 3. Values marked with different upper (Conversion) or lower (Sulphur concentration) cases are significantly different at a 95% confidence level.

T [°C]	t [min]	Conversion [%] <sup>a</sup>			Residual sulphur concentration into heptane solution of benzothiophene [ppm] <sup>b</sup>		
		Biosolids-based catalyst <sup>c,d</sup>	FeCl <sub>3</sub> <sup>c,d</sup>	Non-catalytic system <sup>d</sup>	Biosolids-based catalyst <sup>c,d</sup>	FeCl <sub>3</sub> <sup>c,d</sup>	Non-catalytic system <sup>d</sup>
80	180	>99 <sup>(A)</sup>	95.4 ± 0.7 <sup>(B)</sup>	85.5 ± 0.6 <sup>(D)</sup>	<2 <sup>(a)</sup>	11.5 ± 0.1 <sup>(c)</sup>	36.4 ± 0.3 <sup>(i)</sup>
	120	96.0 ± 0.7 <sup>(B)</sup>	94.7 ± 0.8 <sup>(BC)</sup>	80.5 ± 0.8 <sup>(EF)</sup>	10.0 ± 0.1 <sup>(b)</sup>	13.3 ± 0.1 <sup>(cd)</sup>	48.9 ± 0.5
	60	91.6 ± 0.7 <sup>(C)</sup>	92.5 ± 0.6 <sup>(C)</sup>	77.3 ± 0.8 <sup>(F)</sup>	21.1 ± 0.2 <sup>(f)</sup>	18.8 ± 0.1 <sup>(e)</sup>	57.0 ± 0.6 <sup>(m)</sup>
	30	85.4 ± 1.1 <sup>(D)</sup>	85.0 ± 1.3 <sup>(D)</sup>	55.4 ± 1.0 <sup>(M)</sup>	36.6 ± 0.5 <sup>(i)</sup>	37.7 ± 0.6 <sup>(i)</sup>	111.9 ± 2.0 <sup>(x)</sup>
	15	78.1 ± 0.9 <sup>(F)</sup>	76.6 ± 0.9 <sup>(F)</sup>	49.1 ± 0.9 <sup>(O)</sup>	55.0 ± 0.6 <sup>(m)</sup>	58.7 ± 0.7 <sup>(n)</sup>	127.8 ± 2.3 <sup>(y)</sup>
70	180	>99 <sup>(A)</sup>	92.4 ± 0.9 <sup>(C)</sup>	83.5 ± 0.8 <sup>(DE)</sup>	<2 <sup>(a)</sup>	19.1 ± 0.2 <sup>(e)</sup>	41.4 ± 0.4 <sup>(i)</sup>
	120	96.1 ± 1.1 <sup>(B)</sup>	87.0 ± 1.4 <sup>(D)</sup>	78.5 ± 1.3 <sup>(F)</sup>	9.8 ± 0.11 <sup>(b)</sup>	32.6 ± 0.5 <sup>(g)</sup>	54.0 ± 0.9 <sup>(m)</sup>
	60	86.5 ± 1.2 <sup>(D)</sup>	83.5 ± 1.2 <sup>(DE)</sup>	61.1 ± 1.4 <sup>(L)</sup>	33.9 ± 0.5 <sup>(h)</sup>	41.4 ± 0.6 <sup>(j)</sup>	97.6 ± 2.2 <sup>(v)</sup>
	30	82.9 ± 0.8 <sup>(DE)</sup>	80.9 ± 0.6 <sup>(E)</sup>	55.4 ± 0.5 <sup>(M)</sup>	42.9 ± 0.4 <sup>(k)</sup>	47.9 ± 0.4 <sup>(l)</sup>	111.9 ± 1.0 <sup>(x)</sup>
	15	76.7 ± 0.4 <sup>(FG)</sup>	73.3 ± 1.2 <sup>(GH)</sup>	48.3 ± 1.2 <sup>(O)</sup>	58.5 ± 0.3 <sup>(n)</sup>	67.0 ± 1.1 <sup>(p)</sup>	129.8 ± 3.2 <sup>(w)</sup>
60	180	>99 <sup>(A)</sup>	68.4 ± 0.9 <sup>(J)</sup>	62.4 ± 0.9 <sup>(L)</sup>	<2 <sup>(a)</sup>	79.3 ± 1.0 <sup>(r)</sup>	94.4 ± 1.4 <sup>(u)</sup>
	120	80.6 ± 1.2 <sup>(E)</sup>	67.9 ± 0.7 <sup>(J)</sup>	60.4 ± 0.7 <sup>(L)</sup>	48.7 ± 0.7 <sup>(l)</sup>	80.6 ± 0.8 <sup>(s)</sup>	99.4 ± 1.2 <sup>(v)</sup>
	60	75.4 ± 0.6 <sup>(G)</sup>	65.9 ± 1.3 <sup>(K)</sup>	53.7 ± 1.5 <sup>(MN)</sup>	61.7 ± 0.5 <sup>(o)</sup>	85.6 ± 1.7 <sup>(t)</sup>	116.2 ± 3.2 <sup>(x)</sup>
	30	63.9 ± 1.1 <sup>(K)</sup>	61.8 ± 0.9 <sup>(KL)</sup>	44.7 ± 0.6 <sup>(P)</sup>	90.6 ± 1.6	95.9 ± 1.4 <sup>(u)</sup>	138.8 ± 1.9 <sup>(z)</sup>
	15	56.7 ± 0.7 <sup>(M)</sup>	55.1 ± 0.8 <sup>(M)</sup>	40.6 ± 0.8 <sup>(Q)</sup>	108.7 ± 1.3 <sup>(x)</sup>	112.7 ± 1.6 <sup>(x)</sup>	149.1 ± 2.9 <sup>(aa)</sup>
50	180	86.6 ± 0.6 <sup>(D)</sup>	54.6 ± 1.1 <sup>(M)</sup>	42.4 ± 1.1 <sup>(Q)</sup>	33.6 ± 0.2 <sup>(h)</sup>	114.0 ± 2.3 <sup>(x)</sup>	144.6 ± 3.8 <sup>(aa)</sup>
	120	71.0 ± 1.2 <sup>(H)</sup>	51.1 ± 1.3 <sup>(N)</sup>	40.5 ± 0.8 <sup>(Q)</sup>	72.8 ± 1.2 <sup>(q)</sup>	122.7 ± 3.1 <sup>(y)</sup>	149.3 ± 3.0 <sup>(aa)</sup>
	60	63.4 ± 0.9 <sup>(KL)</sup>	44.1 ± 0.8 <sup>(P)</sup>	39.3 ± 1.2 <sup>(Q)</sup>	91.9 ± 1.3 <sup>(u)</sup>	140.3 ± 2.5 <sup>(z)</sup>	152.4 ± 4.7 <sup>(aa)</sup>
	30	54.2 ± 0.8 <sup>(M)</sup>	41.6 ± 1.2 <sup>(Q)</sup>	30.2 ± 0.9 <sup>(T)</sup>	115.0 ± 1.7 <sup>(x)</sup>	146.6 ± 4.2 <sup>(aa)</sup>	175.2 ± 5.2 <sup>(bb)</sup>
	15	52.1 ± 0.7 <sup>(N)</sup>	38.8 ± 0.5 <sup>(R)</sup>	29.8 ± 0.5 <sup>(T)</sup>	120.2 ± 1.6 <sup>(y)</sup>	153.6 ± 2.0 <sup>(aa)</sup>	176.2 ± 3.0 <sup>(bb)</sup>

<sup>a</sup> Calculated as follow:  $100 \cdot (1 - ((\text{mass of benzothiophene in heptane solution before catalysis} - \text{mass of benzothiophene into heptane solution after catalysis}) / (\text{mass of benzothiophene into heptane solution before catalysis})))$ .

<sup>b</sup> Calculated as follow:  $\text{mass of sulphur into heptane solution before catalysis} - (\text{mass of sulphur into heptane solution before catalysis} \cdot \text{Conversion})$ . Mass of sulphur was calculated accordingly with the elemental analysis of benzothiophene (C = 71.60%; H = 4.51%; S = 23.89%).

<sup>c</sup> Fe/Sulphur = 0.05 mol/mol.

<sup>d</sup> H<sub>2</sub>O<sub>2</sub>/Sulphur = 10 mol/mol.

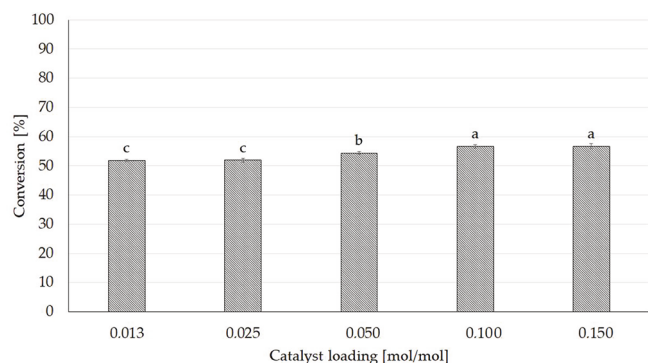


**Fig. 5.** Influence of catalyst loading (reported as ratio between the moles of iron in the biosolids-based material and moles of sulphur) on conversion of benzothiophene solution in heptane at 50 °C for 15 min. The error bars represent the standard deviation calculated according to the values of three catalytic runs. Data annotated with different letters are significantly different at a 95% confidence level. Conversion was calculated as follow:  $100 \cdot [(\text{mass of benzothiophene into heptane solution before catalysis} - \text{mass of benzothiophene into heptane solution after catalysis}) / (\text{mass of benzothiophene into heptane solution before catalysis})]$ .

the recycled catalyst (Fig. 2B), the organic fraction did not undergo any appreciable alterations after the fourth catalytic cycle, but the concentrations of Ti, Zn, Cu, and Mn were drastically decreased (Table 1). Thus, in the fourth catalytic cycle, the performance of the biosolids-based catalyst could be ascribed mostly to the combined activity of iron and aluminum whose concentrations remained stable after the third catalytic run.

### 3.3. Comparative catalytic studies using hydrolysed fatty acids and crude pyrolysis oil recovered from a two-step thermal conversion process using brown grease and biosolids

As demonstrated by our group in the past, biosolids could be incorporated as a water replacement for the two-step thermal conversion of waste fats to renewable hydrocarbons [18,38]. However, this substitution resulted in an increased concentration of sulphur, both within the hydrolysed fatty acids isolated from hydrolysis (step one) and in the crude oil produced through pyrolysis (step two). Bartoli et al. [19] reported a comprehensive study about the behaviour of sulphur during the pyrolysis of hydrolyzed brown grease and applied several non-catalytic desulphurization methodologies to decrease the sulphur levels in the products of both steps. In this section, the catalytic oxidative desulphurization of the hydrolysed fatty acids and crude pyrolysis oil recovered from a two-step thermal conversion process using brown grease and biosolids will be assessed to evaluate the effectiveness of the biosolid-based catalyst and the results are shown in Table 3.

Sulphur compounds in the hydrolyzed fatty acid and crude pyrolysis oil were present mainly as low oxidation state compounds (i.e. thiols, thioethers) [19] whose removal through their conversion to sulfone species is more difficult than benzothiophenes [21]. The treatment of both hydrolysed fatty acids and crude pyrolysis oils at 80 °C for 3 h, but without any catalyst addition, led to poor desulphurization of  $39.6 \pm 0.4$  % and  $10.7 \pm 1.8$  %, respectively. Thus, the desulphurization promoted by the biosolids-based catalyst was generally lower as compared to those achieved using the benzothiophene solution (Table 2). At 70 °C, desulphurization of hydrolyzed fatty acids achieved a conversion of  $87.7 \pm 3.0$  % with a final sulphur concentration of  $61 \pm 3$  ppm. A further increase of temperature to 80 °C did not significantly affect the conversion ( $57 \pm 2$  ppm at 80 °C after 3 h). Hydrolyzed fats recovered after the catalytic oxidative desulphurization were analyzed through gas chromatographic analysis but no alterations due to side reactions were detected. Taking into account the decrease of sulphur promoted by the pyrolytic treatment, oxidative desulphurization may be used as

**Table 3**

Catalytic performance of the solid recovered after hydrolysis of biosolids in the oxidative desulphurization of hydrolysed fatty acids and crude pyrolysis oil recovered from a two-step thermal conversion process using brown grease and biosolids (180 min, Fe/sulphur ratio of 0.05 mol/mol, H<sub>2</sub>O<sub>2</sub>/sulphur ratio of 10/1 mol/mol). The errors represent the standard deviations calculated according to the values of three catalytic runs. Values marked with different upper (Sulphur concentration)/lower case (conversion) are significantly different from each other (confidence level of 95%).

Feedstock	Sulphur concentration Before catalysis [ppm]	H <sub>2</sub> O <sub>2</sub> Sulphur concentration [ppm]	Conversion <sup>a</sup> [%]	Biosolid based catalyst Sulphur concentration [ppm]	Conversion <sup>a</sup> [%]
Hydrolysed fatty acids	80	465 ± 6 <sup>(A)</sup>	281 ± 11 <sup>(D)</sup>	57 ± 2 <sup>(J)</sup>	87.7 ± 0.4 <sup>(a)</sup>
	70		308 ± 2 <sup>(C)</sup>	61 ± 3 <sup>(L)</sup>	86.9 ± 0.6 <sup>(a)</sup>
	60		432 ± 11 <sup>(B)</sup>	84 ± 3 <sup>(H)</sup>	81.9 ± 0.6 <sup>(b)</sup>
Crude pyrolysis oil	50		440 ± 12 <sup>(B)</sup>	134 ± 9 <sup>(F)</sup>	71.2 ± 1.9 <sup>(d)</sup>
	80	253 ± 16 <sup>(E)</sup>	226 ± 13 <sup>(E)</sup>	64 ± 4 <sup>(I)</sup>	74.7 ± 1.1 <sup>(c)</sup>
	70		224 ± 15 <sup>(E)</sup>	96 ± 6 <sup>(G)</sup>	62.1 ± 1.7 <sup>(e)</sup>
	60		234 ± 12 <sup>(E)</sup>	106 ± 5 <sup>(G)</sup>	58.1 ± 1.4 <sup>(e)</sup>
	50		240 ± 9 <sup>(E)</sup>	137 ± 7 <sup>(F)</sup>	45.8 ± 2.0 <sup>(f)</sup>

<sup>a</sup> Calculated as follow:  $100 \times ((\text{concentration of sulphur before catalysis} - \text{concentration of sulphur after catalysis}) / (\text{concentration of sulphur before catalysis}))$ .

pretreatment prior the pyrolytic conversion of the hydrolysed fats.

Desulphurization of crude pyrolysis oil was less effective (74.7 ± 9.5%) with a final concentration achieved of 64 ± 4 ppm at 80 °C, which exceeded the maximum limit allowed for engine fuels [20]. According to Bartoli et al. [19], during pyrolysis, sulphur compounds undergo radical rearrangements forming benzothiophenes, which should theoretically improve the oxidative desulphurization. One explanation for the low effectiveness of the oxidative desulphurization treatment may be that an enhancement in the solubility of oxidized benzothiophenes and high boiling point of sulphur-containing compounds in the crude pyrolysis oil led to the prevalence of aromatics and unsaturated compounds. The aromatic content of crude pyrolysis oil was significantly decreased by the catalytic desulphurization process as shown in Table 4. We observed a relevant decrement of aromatics from 9.5 ± 0.6 wt% to 5.3 ± 0.7 wt% by increasing the reaction temperature to 80 °C. This could be due to the partial oxidation of small aromatics molecules to hydrosoluble compounds [49]. The results also show a significant decrease in the non-aromatic hydrocarbons content after catalysis. There was a concurrent increase in the fatty acids content of the crude pyrolysis oil after catalysis. This increase could be due to concentration effect with the loss of aromatic compounds and non aromatic hydrocarbons by partial oxidation of these species with a subsequent extraction together with the oxidized sulphur species.

#### 4. Conclusions

In this work, we showed that the solid residue recovered after the hydrolysis of biosolids can be used for catalytic oxidative desulphurization due to its high content of metals, predominantly iron and aluminum. Tests conducted using a model fuel solution containing benzothiophene (500 ppm of sulphur) showed a remarkable conversion, with near complete removal of benzothiophene after 3 h at 60 °C. Moreover, the comparison between the biosolids-based catalyst, FeCl<sub>3</sub> and a non-catalytic system demonstrated the superior performance of the former at low reaction time and temperature. The catalytic systems showed a levelling off of activity as the temperature increased and at 80 °C they were not significantly different from each other. The improved performance observed using the biosolids-based catalysts could likely be ascribed to the synergistic effects of aluminium species.

Treatment of crude pyrolysis oil using the biosolids-based catalyst led to a desulfurization of 74.7 ± 9.5 % after 3 h at 80 °C, which corresponded with a final sulphur concentration of 64 ± 4 ppm, a level higher than the maximum tolerated amount of 15 ppm for diesel type fuels. However, desulphurization of hydrolyzed fatty acids recovered from the hydrolytic step of the two-stage thermal conversion of brown grease and biosolids displayed a significantly better conversion (87.7 ± 3.0%). The presence of multiple metal centers such as aluminum,

**Table 4**

The main organic components in the crude pyrolysis oil after catalytic oxidative desulfurization at 80 °C for 3 h using the biosolids-based catalyst. The errors represent the standard deviations calculated from the values of three replicates. Values marked with different capital letters are significantly different from each other (confidence level of 95%).

Composition of crude pyrolysis oil	Total Aromatic compounds [wt%]	Unreacted fatty acids [wt%]	Total non aromatic hydrocarbons [wt%]
Before catalysis	9.5 ± 0.6 <sup>(A)</sup>	23.2 ± 0.8 <sup>(F)</sup>	55.3 ± 0.9 <sup>(G)</sup>
After catalysis at 50 °C	6.5 ± 0.8 <sup>(B)</sup>	27.5 ± 0.7 <sup>(E)</sup>	52.4 ± 1.2 <sup>(H)</sup>
After catalysis at 60 °C	6.6 ± 0.9 <sup>(B)</sup>	28.0 ± 0.9 <sup>(E)</sup>	51.5 ± 1.1 <sup>(H)</sup>
After catalysis at 70 °C	6.0 ± 0.5 <sup>(B)</sup>	28.4 ± 1.1 <sup>(E)</sup>	50.7 ± 0.6 <sup>(H)</sup>
After catalysis at 80 °C	5.3 ± 0.7 <sup>(C)</sup>	32.5 ± 0.7 <sup>(D)</sup>	51.3 ± 0.7 <sup>(H)</sup>

copper, and titanium together with silica-like materials reasonably improved the activity of the complex biosolids-based catalyst in the treatment of recalcitrant sulphur-rich fraction with appreciable, but limited, loss of aromatic molecules. Furthermore, the organic fraction could facilitate the phase transfer of sulphone derivatives from the organic phase to aqueous phase.

Thus, when biosolids are used as a water replacement for the hydrolysis of brown grease, desulphurization of the resulting fatty acids using a biosolids-based catalyst could enable production of a fuel stream that meets the sulphur standards for diesel fuels.

#### Declaration of Competing Interest

The authors declare that they have no known competing financial interests or personal relationships that could have appeared to influence the work reported in this paper.

#### Acknowledgement

We would also like to extend our gratitude to the Natural Resources Analytical Laboratory (Chemistry department, University of Alberta), NanoFab (Engineering faculty, University of Alberta) and to the City of Edmonton, EPCOR Water Services Inc., and Suez for their support throughout the project.

#### Funding

This work was supported through generous contributions from the

Natural Sciences and Engineering Research Council of Canada (NSERC) [grant number RGPIN 298352–2013], Mitacs Canada [grant number MI MA IT05367], BioFuelNet Canada [grant number NCEBFC 6F], Agriculture and Agri-Food Canada's Canadian Agricultural Partnership [Bressler AgriScience Cluster project], and our collaborators from Forge Hydrocarbons Inc. who also hosted Mattia Bartoli as an intern.

## Bibliography

- [1] Choudhary M, Peter C, Shukla SK, Govender PP, Joshi GM, Wang R. Environmental issues: a challenge for wastewater treatment. *Green Materials for Wastewater Treatment* Springer 2020:1–12.
- [2] Ramalho R. Introduction to wastewater treatment processes. Elsevier; 2012.
- [3] Tchobanoglous G, Burton FL. *Wastewater engineering Management* 1991;7:1–4.
- [4] Agency USEP. <https://www.epa.gov/biosolids>; 2017. 2018].
- [5] Sommers LE. Chemical composition of sewage sludges and analysis of their potential use as fertilizers. *J Environ Qual* 1977;6(2):225–32.
- [6] McFarland MJ. *Biosolids engineering*. McGraw-Hill Professional Publishing; 2000.
- [7] Oleszczuk P, Baran S. Application of solid-phase extraction to determination of polycyclic aromatic hydrocarbons in sewage sludge extracts. *J Hazard Mater* 2004; 113(1-3):237–45.
- [8] Golet EM, Strehler A, Alder AC, Giger W. Determination of fluoroquinolone antibacterial agents in sewage sludge and sludge-treated soil using accelerated solvent extraction followed by solid-phase extraction. *Anal Chem* 2002;74(21): 5455–62.
- [9] Berrow ML, Webber J. Trace elements in sewage sludges. *J Sci Food Agric* 1972;23 (1):93–100.
- [10] SMITH S. A critical review of the bioavailability and impacts of heavy metals in municipal solid waste composts compared to sewage sludge. *Environ Int* 2009;35 (1):142–56.
- [11] Mateo-Sagasta J, Raschid-Sally L, Thebo A. Global Wastewater and Sludge Production, Treatment and Use. In: Drechsel P, Qadir M, Wichelns D, editors. *Wastewater: Economic Asset in an Urbanizing World*. Dordrecht: Springer, Netherlands; 2015. p. 15–38.
- [12] HARGREAVES J, ADL M, WARMAN P. A review of the use of composted municipal solid waste in agriculture. *Agric Ecosyst Environ* 2008;123(1-3):1–14.
- [13] Sarafadeen AO, Aderonke O, Enitan AF, Olusegun OA, Oluwasegun A. Biosolids land applications. *Pensee* 2014;76:9.
- [14] Kalavrouziotis IK. *Wastewater and biosolids management*. London, United Kingdom: IWA Publishing; 2020.
- [15] Wang H, Brown SL, Magesan GN, Slade AH, Quintern M, Clinton PW, et al. Technological options for the management of biosolids. *Environmental Science and Pollution Research-International* 2008;15(4):308–17.
- [16] Bhatta Kaudal B, Aponte C, Brodie G. Biochar from biosolids microwaved-pyrolysis: Characteristics and potential for use as growing media amendment. *J Anal Appl Pyrol* 2018;130:181–9.
- [17] Molla AH, Fakhru'l-Razi A, Hanafi MM, Alam MZ. Compost produced by solid state bioconversion of biosolids: A potential resource for plant growth and environmental friendly disposal. *Commun Soil Sci Plant Anal* 2005;36(11-12): 1435–47.
- [18] Omidghane M, Bartoli M, Asomaning J, Xia L, Chae M, Bressler DC. Pyrolysis of fatty acids derived from hydrolysis of brown grease with biosolids. *Environ Sci Pollut Res* 2020;27(21):26395–405.
- [19] Bartoli M, Asomaning J, Xia L, Chae M, Bressler DC. Desulfurization of drop-in fuel produced through lipid pyrolysis using brown grease and biosolids feedstocks. *Biomass Bioenergy* 2021;154:106233. <https://doi.org/10.1016/j.biombioe.2021.106233>.
- [20] Iruretagoyena D, Montesano R. *Selective Sulfur Removal from Liquid Fuels Using Nanostructured Adsorbents*. Nanotechnology in Oil and Gas Industries Springer 2018:133–50.
- [21] Zeelani GG, Ashrafi A, Dhakad A, Gupta G, Pal SL. Catalytic Oxidative desulfurization of liquid fuels. A review 2016.
- [22] Murata S, Murata K, Kidena K, Nomura M. A novel oxidative desulfurization system for diesel fuels with molecular oxygen in the presence of cobalt catalysts and aldehydes. *Energy Fuels* 2004;18(1):116–21.
- [23] Yan X-M, Mei P, Lei J, Mi Y, Xiong L, Guo L. Synthesis and characterization of mesoporous phosphotungstic acid/TiO<sub>2</sub> nanocomposite as a novel oxidative desulfurization catalyst. *J Mol Catal A: Chem* 2009;304(1):52–7.
- [24] Sampanthar JT, Xiao H, Dou J, Nah TY, Rong Xu, Kwan WP. A novel oxidative desulfurization process to remove refractory sulfur compounds from diesel fuel. *Appl Catal B* 2006;63(1-2):85–93.
- [25] Tamborrino V, Costamagna G, Bartoli M, Rovere M, Jagdale P, Lavagna L, et al. Catalytic oxidative desulfurization of pyrolytic oils to fuels over different waste derived carbon-based catalysts. *Fuel* 2021;296:120693. <https://doi.org/10.1016/j.fuel.2021.120693>.
- [26] Trakampruk W, Rujiraworawut K. Oxidative desulfurization of gas oil by polyoxometalates catalysts. *Fuel Process Technol* 2009;90(3):411–4.
- [27] Lü H, Gao J, Jiang Z, Yang Y, Song Bo, Li C. Oxidative desulfurization of dibenzothiophene with molecular oxygen using emulsion catalysis. *Chem Commun* 2007;(2):150–2. <https://doi.org/10.1039/B610504A>.
- [28] Zhang W, Zhang H, Xiao J, Zhao Z, Yu M, Li Z. Carbon nanotube catalysts for oxidative desulfurization of a model diesel fuel using molecular oxygen. *Green Chem* 2014;16(1):211–20.
- [29] Collins FM, Lucy AR, Sharp C. Oxidative desulfurization of oils via hydrogen peroxide and heteropolyanion catalysis. *J Mol Catal A: Chem* 1997;117(1-3): 397–403.
- [30] Wang D, Qian EW, Amano H, Okata K, Ishihara A, Kabe T. Oxidative desulfurization of fuel oil: Part I. Oxidation of dibenzothiophenes using tert-butyl hydroperoxide. *Appl Catal A* 2003;253(1):91–9.
- [31] Zhu WenShuai, Li H, Gu QingQing, Wu P, Zhu G, Yan Y, et al. Kinetics and mechanism for oxidative desulfurization of fuels catalyzed by peroxy-molybdenum amino acid complexes in water-immiscible ionic liquids. *J Mol Catal A: Chem* 2011;336(1-2):16–22.
- [32] Haw K-G, Bakar WAWA, Ali R, Chong J-F, Kadir AAA. Catalytic oxidative desulfurization of diesel utilizing hydrogen peroxide and functionalized-activated carbon in a biphasic diesel-acetonitrile system. *Fuel Process Technol* 2010;91(9): 1105–12.
- [33] Zhang M, Zhu W, Xun S, Li H, Gu Q, Zhao Z, et al. Deep oxidative desulfurization of dibenzothiophene with POM-based hybrid materials in ionic liquids. *Chem Eng J* 2013;220:328–36.
- [34] Li C, Jiang Z, Gao J, Yang Y, Wang S, Tian F, et al. Ultra-Deep Desulfurization of Diesel: Oxidation with a Recoverable Catalyst Assembled in Emulsion. *Chemistry-A European Journal* 2004;10(9):2277–80.
- [35] BARB WG, BAXENDALE JH, GEORGE PHILIP, HARGRAVE KR. Reactions of ferrous and ferric ions with hydrogen peroxide. *Nature* 1949;163(4148):692–4.
- [36] Neyens E, Baeyens J. A review of classic Fenton's peroxidation as an advanced oxidation technique. *J Hazard Mater* 2003;98(1-3):33–50.
- [37] Balmér P. *Chemical Treatment — Consequences for Sludge Biosolids Handling*. Berlin, Heidelberg: Springer Berlin Heidelberg; 1994:319-27.
- [38] Xia L, Chae M, Asomaning J, Omidghane M, Zhu C, Bressler DC. Incorporation of Biosolids as Water Replacement in a Two-Step Renewable Hydrocarbon Process: Hydrolysis of Brown Grease with Biosolids. *Waste Biomass Valorization* 2020;11 (12):6769–80.
- [39] Bartoli M, Zhu C, Chae M, Bressler DC. Value-added products from urea glycerolysis using a heterogeneous biosolids-based catalyst. *Catalysts* 2018;8(9): 373.
- [40] Bartoli M, Zhu C, Chae M, Bressler DC. Glycerol Acetylation Mediated by Thermally Hydrolysed Biosolids-Based Material. *Catalysts* 2020;10(1):5–19.
- [41] Asomaning J, Mussone P, Bressler DC. Two-stage thermal conversion of inedible lipid feedstocks to renewable chemicals and fuels. *Bioresour Technol* 2014;158: 55–62.
- [42] Benítez E, Romero E, Gomez M, Gallardo-Lara F, Nogales R. Biosolids and biosolids-ash as sources of heavy metals in a plant-soil system. *Water Air Soil Pollut* 2001;132(1–2):75–87.
- [43] Campos-Martin JM, Capel-Sanchez MC, Perez-Presas P, Fierro JLG. Oxidative processes of desulfurization of liquid fuels. *J Chem Technol Biotechnol* 2010;85(7): 879–90.
- [44] Wang G-J, Zhang J-K, Liu Y. Catalytic oxidative desulfurization of benzothiophene with hydrogen peroxide over Fe/AC in a biphasic model diesel-acetonitrile system. *Korean J Chem Eng* 2013;30(8):1559–65.
- [45] Ganiyu SA, Alhooshani K, Sulaiman KO, Qamaruddin M, Bakare IA, Tanimu A, et al. Influence of aluminium impregnation on activated carbon for enhanced desulfurization of DBT at ambient temperature: Role of surface acidity and textural properties. *Chem Eng J* 2016;303:489–500.
- [46] Herlihy TE. In: *Plant Polyphenols 2*. Boston, MA: Springer US; 2000. p. 791–804. [https://doi.org/10.1007/978-1-4615-4139-4\\_44](https://doi.org/10.1007/978-1-4615-4139-4_44).
- [47] Han N, Thompson ML. Copper-binding ability of dissolved organic matter derived from anaerobically digested biosolids. *J Environ Qual* 1999;28(3):939–44.
- [48] Wang R, Yu F, Zhang G, Zhao H. Performance evaluation of the carbon nanotubes supported Cs<sub>2</sub> 5H<sub>0</sub>. 5PW12O<sub>40</sub> as efficient and recoverable catalyst for the oxidative removal of dibenzothiophene. *Catal Today* 2010;150(1-2):37–41.
- [49] Pignatello JJ, Oliveros E, MacKay A. Advanced oxidation processes for organic contaminant destruction based on the Fenton reaction and related chemistry. *Critical reviews in environmental science and technology* 2006;36(1):1–84.
- [50] Barb WG, Baxendale JH, George P, Hargrave KR. Reactions of ferrous and ferric ions with hydrogen peroxide. Part I.—The ferrous ion reaction. *Transaction of the Faraday Society* 1951;47(0):462–500.
- [51] Barb WG, Baxendale JH, George P, Hargrave KR. Reactions of ferrous and ferric ions with hydrogen peroxide. Part II.—The ferric ion reaction. *Trans Faraday Soc* 1951;47(0):591–616.
- [52] Ensing B, Buda F, Baerends EJ. Fenton-like chemistry in water: oxidation catalysis by Fe (III) and H<sub>2</sub>O<sub>2</sub>. *The Journal of Physical Chemistry A* 2003;107(30):5722–31.
- [53] Ruipérez F, Mujika JI, Ugalde JM, Exley C, Lopez X. Pro-oxidant activity of aluminum: promoting the Fenton reaction by reducing Fe (III) to Fe (II). *J Inorg Biochem* 2012;117:118–23.
- [54] Wei S, He H, Cheng Y, Yang C, Zeng G, Qiu Lu. Performances, kinetics and mechanisms of catalytic oxidative desulfurization from oils. *RSC Adv* 2016;6(105): 103253–69.
- [55] von Sonntag C, Schuchmann H. Peroxyl radicals in aqueous solutions in Peroxyl Radicals. *Alfassi ZB* 1997:174–234.
- [56] Hug SJ, Leupin O. Iron-catalyzed oxidation of arsenic (III) by oxygen and by hydrogen peroxide: pH-dependent formation of oxidants in the Fenton reaction. *Environ Sci Technol* 2003;37(12):2734–42.
- [57] Bhasarkar JB, Chakma S, Moholkar VS. Mechanistic features of oxidative desulfurization using sono-Fenton-peracetic acid (ultrasound/Fe<sub>2</sub>+—CH<sub>3</sub>COOH—H<sub>2</sub>O<sub>2</sub>) system. *Ind Eng Chem Res* 2013;52(26):9038–47.